Published by
NIGERIAN SOCIETY OF PHYSICAL SCIENCES
Available online @ https://journal.nsps.org.ng/index.php/jnsps

J. Nig. Soc. Phys. Sci. 7 (2025) 2896

Journal of the Nigerian Society of Physical Sciences

Eigensolutions and thermodynamic properties constrained by magnetic field of cyclotron frequency

C. A. Onate, S. O. Mobolaji*, J. A. Akinpelu

Department of Physics, Bowen University, Iwo, Nigeria

Abstract

The present work investigates the influence of cyclotron frequency on the energy spectrum and thermodynamic properties of a quantum system. The energy as a function of the quantum number unveils an increase in the system's energy due to the presence of cyclotron frequency, making it open-ended by curtailing its negativity. The screening parameter significantly shapes the system's energy, increasing at the initial point due to Landau quantization and then monotonically decreasing as a result of weakness of Coulomb interaction. The study also revealed that the parameter a and b impacted the energy differently as the cyclotron frequency altering the system's confinement behaviours. Similarly, the partition function (Z) and some thermodynamic properties (TP), are analyzed under varying temperatures and parameter conditions. The presence of the cyclotron frequency (CF) reduces the Z and the TP due to Zeeman effect. The TP (H and S) exhibited similar characteristics. Thus, the presence of CF affects the stability of the system. This study finds applications in quantum wells and dots, fusion energy, magnetic quantum computing, and quantum statistical mechanics.

DOI:10.46481/jnsps.2025.2896

Keywords: Bound state, Eigensolution, Thermal properties, Partition function, Potential model

Article History :
Received: 20 April 2025
Received in revised form: 15 June 2025
Accepted for publication: 04 July 2025
Available online: 25 August 2025

Communicated by: B. J. Falaye

1. Introduction

The study of thermodynamics is essentially dependent of energy which is a fundamental concept governing the behaviour and transformations of some quantum and physical systems. The storage of energy, its transformation and conversion are command by thermodynamics. Thus, thermodynamics study internal energy which comprises of the kinetic energy of particle and the potential energy arising from atomic interaction, thermal energy which is a subset of internal energy usually associated with random motion of particles, work and heat that account for energy transfer due to macroscopic forces and due to temperature gradient. In a deeper understanding, the three laws of thermodynamics revolved around the energy. The non-creation and non-destruction of energy, the dissipation of energy as heat and the deterministic of the entire energy. In the TP such as enthalpy (H), Helmholtz free energy (HFE), Gibbs free energy (G), heat capacities (C_p), and entropy (S), energy is greatly involved. Energy is therefore, the bedrock of thermodynamics, defining the behaviour, limits, and efficiency of all physical and chemical processes. The study of thermodynamic properties in the recent times bridges quantum mechanics and statistical mechanics via energy levels. In quantum mechanics, the study of bound states from potential models leads to energy levels. These energy levels are connected to the thermodynamic properties via partition function. The Z is a key concept in the study of TP via energy levels. It acts as a bridging tool between

*Corresponding author Tel. No.: +234-810-055-5842.
Email address: solomondotyem@gmail.com (S. O. Mobolaji)

the microscopic properties of a system and the macroscopic TP as it encapsulates the statistical distribution of energy. Z as a pillar tool in the study of thermodynamics, providing a quantitative measure of the system's accessibility of microstates at a given temperature. Recent studies reported the various thermodynamic properties (TP) via the Z from energy levels. Edet *et al*. [1], for instance studied some TP under the interaction of a combination of Deng-Fan Eckart potential. Their results revealed similar effects of temperature on the properties. In another development, Okon *et al*. [2], studied the TP for Mobius square plus screened Kratzer potentials. The authors reported different effects of β and λ on the various properties.

Ikot *et al*. [3], reported non-consistence of the effect of β and λ on the various TP for screened Kratzer model. Rampho *et al*. [4] examined the action of magnetic and AB fields on the TP for improved Kratzer potential. The results showed an external behaviours by the various properties due to the magnetic and AB fields. Emeje *et al*. [5] recently studied the various TP under the standard Coulombic potential. The study pointed out the different effects of the β and λ on the various TP. Jiang *et al*. in Ref. [6] studied and reported temperature (T) effect on TP. Their result demonstrates the principle of phase transformations regulated in Fe-C-X alloys. Habibinejad *et al*. [7] calculated TP of boron nitride for a q-deformed exponential-type potential. Their model reproduces experimental data with higher deviation compared to other models. For molecular potential models where the potential parameters have physical definition, several analytical TP have been analyzed and contrasted with the tested data. Such reports can be found in Ref. [8] where Khordad and Ghanbari studied TP of K2 for generalized Mobius square potential and reported the highest deviation of their predicted result from experimental result as 0.01139 at 800K for C_p, 0.07486 at 4000K for H, 0.10017 at 6000K for H and 0.09112 at 5000K for G. Their model performed perfectly for the TP of potassium molecule.

Similarly, Onate *et al*. [9], reported molar S for I_2, SiC, and CP. Their results agreed with experimental data. Their model was tested by calculating average absolute deviation from experimental data that varies from molecule to molecule. Eyube *et al*. [10], reported the molar H and molar G of P_2, N_2 and ICl for improved Pöschl-Teller oscillator. Their results are consistent with the observed data from NIST database. Emeje *et al*. [11], also reported the molar H, molar C_p at constant pressure and molar G of N2 and I2 for a modified shifted Morse potential. Their results are also consistent with the observed data from NIST database. Generally, TP are applicable in dissolution, phase transition, protein activity, material synthesis, fluorescence microscopy as well as adsorption [12–18]. Driven by the curiosity about TP and the energy levels of the exponential-type potential, the study wants to examine the effects of CF (incorporating magnetic field) on the TP. The CF also governs the dynamics of charged particles, influencing transport coefficients like electrical and thermal conductivity. By assumption, we believed that the interaction of the CF may leads to energy absorption and can significantly alter thermodynamic behaviour. The exponential-type potential with the CF takes the form:

$$V(r) = -\frac{a}{1-e^{-\alpha r}} - \frac{b}{(1-e^{-\alpha r})^2} + \frac{1}{2}\frac{m^*\omega_0}{r} + \frac{1}{8}m^*\omega_0^2\hbar, \tag{1}$$

where a and b are potential strengths, m^* is the mass, $\hbar$ is the reduced Planck's constant, and ω_0 is the CF that is equivalent to the product of the magnetic field (B) and the a charge (q) over the mass (m). Mathematically, the CF is given by

$$\omega_c = \frac{qB}{m^*}. \tag{2}$$

Cyclotron frequency is the frequency at which a charged particle rotates in a magnetic field. It is a critical quantity in classical fields and quantum descriptions of charged particle dynamics. The concept reveals how magnetic fields influence particle's paths and energy levels. This frequency acted on a particle with three different parameters as shown in equation (2). Cyclotron frequency bridges electromagnetism that describes the motion of charged particles, and thermodynamics that oversees the macroscopic energy transfer.

2. The parametric Nikiforov-Uvarov (PNU) approach

To obtain the energy levels of any potential model using the methodology of PNU, a standard formula is advocated in Ref. [19] as:

$$\frac{d^2\psi(x)}{dx^2} + \frac{v_1 - v_2 x}{x(1-v_3 x)}\frac{d\psi(x)}{dx} + \frac{-Px^2 + Rx - Q}{x^2(1-v_3 x)^2}\psi(x) = 0. \tag{3}$$

From (3), the energy levels and its wave function can be amassed following the condition:

$$v_2 n - (2n+1)v_5 + n(n-1)v_3 + v_7 + 2v_2 v_8 + (2n+1)(\sqrt{v_9} + v_3\sqrt{v_8}) + 2\sqrt{v_8 v_9} = 0, \tag{4}$$

$$\psi(x) = x^{v_{12}}(1-v_3 x)^{-v_{12}-\frac{v_{13}}{v_3}} P_n^{(v_{10}-1, \frac{v_{11}}{v_3}-v_{10}-1)}(1-2v_3 x). \tag{5}$$

The attributes in equations (4) and (5) are secured as follows:

$$\begin{aligned} &v_4 = 0.5(1-v_1), v_5 = 0.5(v_2 - 2v_3),\\ &v_6 = v_5^2 + P, c_7 = 2v_4 v_5 - R, v_8 = v_4^2 + Q,\\ &v_9 = v_3(v_7 + v_3 v_8) + v_6,\\ &v_{10} = v_1 + 2v_4 + 2\sqrt{v_8},\\ &v_{11} = v_2 - 2v_5 + 2(\sqrt{v_9} + v_3\sqrt{v_8}),\\ &v_{12} = v_4 + \sqrt{v_8}, v_{13} = v_5 - (\sqrt{v_9} + v_3\sqrt{v_8}). \end{aligned} \tag{6}$$

3. Bound state solutions

To study a physical system for any solvable potential model, the radial Schrödinger equation is given as:

$$-\frac{\hbar}{2\mu}\frac{d^2U_{n,\ell}(r)}{dr^2}+\frac{\hbar}{2\mu}\frac{\ell(\ell+1)}{r^2}U_{n,\ell}(r)=E_{n,\ell}U_{n,\ell}(r)-V(r)U_{n,\ell}(r), \tag{7}$$

where $E_{n,\ell}$ is the nonrelativistic energy, $V(r)$ is potential, n is the quantum number, μ is the reduced mass, r is the internuclear separation, ℓ is the angular momentum and $U_{n,\ell}(r)$ is the radial wave function. The inverse squared term in equation (7) can be approximated using [20]:

$$\frac{1}{r^2}\approx\frac{\alpha^2}{(1-e^{-\alpha r})^2}. \tag{8}$$

Inserting equation (1) and equation (8) into equation (3), and make a transformation of variable as $x=e^{-\alpha r}$, the radial equation in equation (7) becomes

$$\begin{aligned}&\frac{d^2U_{n\ell}(x)}{dx^2}+\frac{1-x}{x(1-x)}\frac{dU_{n,\ell}(x)}{dx}\\&+\left[\frac{\rho_0x^2-(2\rho_0+\rho_1)x+\rho_0+\rho_1+\frac{2m^*b}{\alpha^2\hbar^2}-\ell(\ell+1)}{x^2(1-x)^2}\right]\\&\times U_{n,\ell}(x)=0,\end{aligned} \tag{9}$$

where

$$\rho_0=\frac{2mE_{n,\ell}}{\alpha^2\hbar^2}-\frac{m^2\omega_c^2}{4\alpha^2\hbar},\rho_1=\frac{2ma}{\alpha^2\hbar^2}-\frac{m^2\omega_c}{\alpha\hbar^2}. \tag{10}$$

By juxtaposing equation (9) with equation (3), the attributes outlined in equation (6) can be expressed as:

$$\begin{aligned}&v_1=v_2=v_3=1,v_4=0,v_5=-\frac{1}{2},\\&v_6=\frac{1}{4}-\rho_0,c_7=2\rho_0+\rho_1,\\&v_8=-\rho_0-\rho_0+\ell(\ell+1)-\frac{2mb}{\alpha^2\hbar^2},\\&v_9=\ell(\ell+1)+\frac{1}{4}-\frac{2mb}{\alpha^2\hbar^2},\\&v_{10}=1+2\sqrt{\ell(\ell+1)-\rho_0-\rho_0-\frac{2mb}{\alpha^2\hbar^2}},\\&v_{12}=\sqrt{\ell(\ell+1)-\rho_0-\rho_0-\frac{2mb}{\alpha^2\hbar^2}},\\&v_{11}=2(1+\sqrt{\ell(\ell+1)-\rho_0-\rho_0-\frac{2mb}{\alpha^2\hbar^2}}+\\&\sqrt{(1+2\ell)^2-\frac{8mb}{\alpha^2\hbar^2}},\\&v_{13}=-\frac{1}{2}-\frac{1}{2}\sqrt{(1+2\ell)^2-\frac{8mb}{\alpha^2\hbar^2}}-\\&\sqrt{\ell(\ell+1)-\rho_0-\rho_0-\frac{2mb}{\alpha^2\hbar^2}}\end{aligned} \tag{11}$$

Plugging $v_i(i=1,2,3,...,9)$ and $v_{ii}(ii=10,11,12,13)$ into equation (4) and equation (5) respectively, the energy levels and the wave function for equation (1) becomes:

$$\begin{aligned}E_{n,\ell}=\theta_0+\frac{\ell(\ell+1)\alpha^2\hbar^2}{2m}-\frac{\alpha^2\hbar^2}{2m}\times\\\left[\frac{\theta_{01}-n(n+1)-(n+\frac{1}{2})\sqrt{(1+2\ell)^2-\frac{8mb}{\alpha^2\hbar^2}}}{2n+1+\sqrt{(1+2\ell)^2-\frac{8mb}{\alpha^2\hbar^2}}}\right]^2,\end{aligned} \tag{12}$$

$$R_{n,\ell}(x)=Nx^{\theta_{11}}(1-x)^{\frac{1}{2}+\frac{1}{2}\theta_2}P_n^{2\theta_{11},\theta_2}(1-2x), \tag{13}$$

where

$$\begin{aligned}\theta_0&=\frac{m\hbar\omega_c^2}{8}+\frac{m\alpha\omega_c}{2}-\alpha a-b,\\\theta_{01}&=\frac{2m(a+2b)}{\alpha^2\hbar^2}-\frac{m^2\omega_c}{\alpha\hbar^2}-\frac{1}{2}-2\ell(\ell+1),\\\theta_{11}&=\sqrt{\ell(\ell+1)-\rho_0-\rho_0-\frac{2mb}{\alpha^2\hbar^2}},\end{aligned} \tag{14}$$

4. Computation of the vibrational partition function (Z) and TP

At this point, we can now calculate the Z using the Poisson summation formula. The computation of the Z is purely vibrational. The Z and the pure energy level are related by the formula [21–29]

$$Z=\sum_{n=0}^{n_{max}}e^{-\beta E_n}. \tag{15}$$

Plugging equation (12) into equation (15) to have

$$Z=e^{-\beta\theta_0}\sum_{n=0}^{n_{max}}e^{\beta E_n}, \tag{16}$$

where

$$E_n=\theta_0-\frac{\alpha^2\hbar^2}{2m}\left[\frac{\frac{2\theta_1-\theta_2}{2}-n(n+1+\theta_2}{2n+1+\theta_2}\right]^2. \tag{17}$$

$$\theta_1=\frac{2m(a+2b)}{\alpha^2\hbar^2}-\frac{m^2\omega_c}{\alpha\hbar^2}-\frac{1}{2},\theta_2=\sqrt{1-\frac{8mb}{\alpha^2\hbar^2}}. \tag{18}$$

Using Poisson summation formula [30–35], equation (16) becomes

$$\begin{aligned}Z=e^{-\beta\theta_0}\sum_{n=0}^{n_{max}}e^{\beta E_n}=e^{-\beta\theta_0}\sum_{n=0}^{n_{max}}f(n)=\\e^{-\beta\theta_0}\left\{\frac{1}{2}(f(0)-f(n_{max}+1))+\int_0^{n_{max}+1}f(x)dx\right\}.\end{aligned} \tag{19}$$

The n_{max} is the maximum vibrational quantum state while $\beta=(k_{\beta T})^{-1}$ with k_β as the Boltzmann constant and T is the absolute temperature. From equation (17), the maximum vibrational quantum state is obtained as:

$$n_{max}=\frac{1}{2}+\frac{1}{2}\theta_2-\frac{1}{2}\sqrt{-(\theta_2^2+4\theta_1+1)}. \tag{20}$$

Using equation (17) in equation (19) for terms under summation, we have:

$$\sum_{n=0}^{n_{max}} = \frac{1}{2}\left(e^{\theta^2\theta_3^2} - e^{\theta^2\theta_4^2}\right) + \int_0^{n_{max}+1} e^{\theta^2\left(\frac{\theta_1 - x(x+1) - (x+0.5)\theta_2}{2x+1+\theta_2}\right)^2} dx, \quad (21)$$

where

$$\theta_2 = \frac{\beta\alpha^2\hbar^2}{2m}, \theta_3 = \frac{\theta_1 - 0.5\theta_2}{1+\theta_2}, \\ \theta_4 = \frac{\theta_1 - (n_{max}+1)(n_{max}+2) - (n_{max}+1.5)\theta_2}{2n_{max}+3+\theta_2}. \quad (22)$$

Defining

$$\theta_5 = \theta\left(\frac{\theta_1 - x(x+1) - (x+0.5)\theta_2}{2x+1+\theta_2}\right), \quad (23)$$

the integral in equation (21) turns out to be:

$$\int_0^{n_{max}+1} e^{\theta^2\left(\frac{\theta_1 - x(x+1) - (x+0.5)\theta_2}{2x+1+\theta_2}\right)^2} dx = \\ \frac{1}{\theta}\int_{\theta_3}^{\theta_4} e^{\theta_5^2} d\theta_5 - \frac{1}{\theta}\int_{\theta_3}^{\theta_4} \frac{2\theta_5}{\sqrt{4\theta_5^2 + \theta^2 + \theta^2\theta_2^2}} e^{\theta_5^2} d\theta_5. \quad (24)$$

Using maple software program, the complete partition function for the system becomes:

$$Z = \frac{e^{-\beta\theta_0}}{2}\left\{e^{\theta^2\theta_3^2} - e^{\theta^2\theta_4^2} + \frac{\sqrt{\pi}[erfi(\theta_6) - erfi(\theta_7) - erfi(\theta_4) - erfi(\theta_3)]}{\theta}\right\}, \quad (25)$$

$$\theta_6 = \frac{1}{2}\sqrt{4\theta_4^2 + \theta^2(1+\theta_2^2)}, \\ \theta_7 = \frac{1}{2}\sqrt{4\theta_3^2 + \theta^2(1+\theta_2^2)}. \quad (26)$$

It is noted that the TP are calculated from the Z and its derivatives. Having obtained the Z, it becomes easier to calculate the TP such as the enthalpy and entropy [36].

4.1. Vibrational enthalpy (H)

The vibrational H is given by

$$H = \frac{T}{\beta}\frac{\partial \ln Z}{\partial T}. \quad (27)$$

Plugging equation (25) into equation (27), the H becomes

$$H = \frac{\theta_0 e^{-\beta\theta_0}\left\{\frac{1}{2}e^{\theta^2\theta_3^2} - \frac{1}{2}e^{\theta^2\theta_4^2} - \frac{\sqrt{2}\theta_{10}}{2\theta}\right\}}{e^{-\beta\theta_0}\left\{\frac{1}{2}e^{\theta^2\theta_3^2} - \frac{1}{2}e^{\theta^2\theta_4^2} - \frac{\theta_{10}}{\theta}\right\}} + \\ \frac{e^{-\beta\theta_0}\left\{\frac{\theta^2 e^{\theta^2}\theta_T}{2T} - \frac{\theta_{11}}{\theta} + e^{-\frac{\theta^2}{4}(1+\theta_2^2)}\theta_{12}\frac{\sqrt{\pi}}{\theta}\right\}}{e^{-\beta\theta_0}\left\{\frac{1}{2}e^{\theta^2\theta_3^2} - \frac{1}{2}e^{\theta^2\theta_4^2} - \frac{\theta_{10}}{\theta}\right\}} \\ - \frac{\frac{\beta\theta_{13}\left(\sqrt{\beta m^{-1}}\right)^{-3/2}}{4\alpha\hbar mT}}{e^{-\beta\theta_0}\left\{\frac{1}{2}e^{\theta^2\theta_3^2} - \frac{1}{2}e^{\theta^2\theta_4^2} - \frac{\theta_{10}}{\theta}\right\}}, \quad (28)$$

$$\theta_8 = \frac{1}{4}\sqrt{16\theta_3^2 + \frac{2\alpha^2\hbar^2(1+\theta_2^2)}{k_\beta mT}}, \\ \theta_9 = \frac{1}{4}\sqrt{16\theta_4^2 + \frac{2\alpha^2\hbar^2(1+\theta_2^2)}{k_\beta mT}}. \quad (29)$$

$$\theta_{10} = e^{-\theta^2\left(\frac{1+\theta_2^2}{4}\right)}\sqrt{2\pi}\left[erfi(\theta_8) + erfi(\theta_9) - erfi(\theta_4) - erfi(\theta_3)\right], \quad (30)$$

$$\theta_{11} = \left(\frac{\theta^2 + \theta^2\theta_2^2}{4}\right)e^{-\frac{\theta^2+\theta^2\theta_2^2}{4}}\sqrt{\pi}\left[erfi(\theta_8) + erfi(\theta_9)\right], \quad (31)$$

$$\theta_{12} = \frac{e^{\theta_3^2 - \frac{\theta^2 - \theta^2\theta_2^2}{4}}\left(-\frac{2\alpha^2\hbar^2\beta(1+\theta_2^2)}{mT}\right)}{4\theta_8\sqrt{\pi}} + \\ \frac{e^{-\theta_4^2 - \frac{\theta^2 - \theta^2\theta_2^2}{4}}\left(-\frac{2\alpha^2\hbar^2\beta(1+\theta_2^2)}{mT}\right)}{4\theta_9\sqrt{\pi}}, \quad (32)$$

$$\theta_{13} = e^{-\frac{\theta^2+\theta^2\theta_2^2}{4}}\sqrt{2\pi}\left[erfi(\theta_8) + erfi(\theta_8) - erfi(\theta_4) - erfi(\theta_3)\right]. \quad (33)$$

4.2. Vibrational entropy (S)

$$S = \frac{1}{\beta T}\ln Z + \frac{1}{\beta}\frac{\partial \ln Z}{\partial T}. \quad (34)$$

Plugging equation (25) into equation (34) gives

$$S = k_\beta \ln\left\{\frac{e^{-\beta\theta_0}}{2}\left(e^{\theta^2\theta_3^2} - e^{\theta^2\theta_4^2} + \frac{\sqrt{\pi}[erfi(\theta_6) - erfi(\theta_7) + erfi(\theta_4) - erfi(\theta_3)]}{\theta}\right)\right\} + \frac{H}{T}. \quad (35)$$

4.3. Vibrational Gibbs free energy (G)

$$G = H - TS \equiv -RT\ln Z. \quad (36)$$

4.4. Vibrational heat capacity (C)

$$C = \frac{\partial H}{\partial T} \quad (37)$$

5. Discussion

The energy of the system versus n is shown in Figure 1. The red colour represents energy with the effect of CF while the blue colour stands for energy without the effect of CF. The relationship between energy and n is considered for larger n to examine a proper variation of energy and effect of the CF. The n exhibits the same effect on the energy with CF and without the effect of CF. The presence of CF increases the energy making the energy of the system less bounded as electrons are loosely

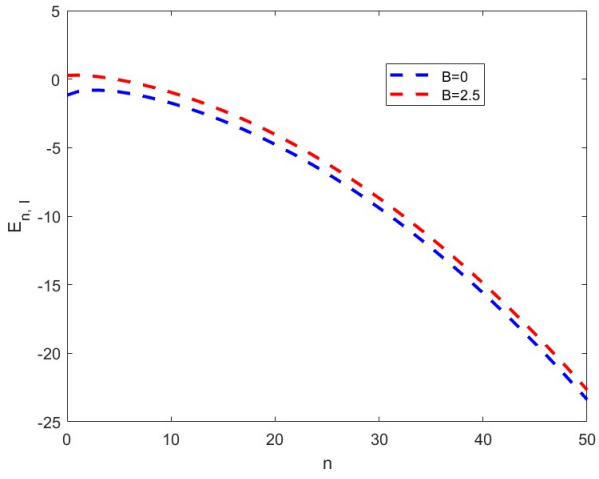

Figure 1: $E_{n,\ell}$ of the system versus n.

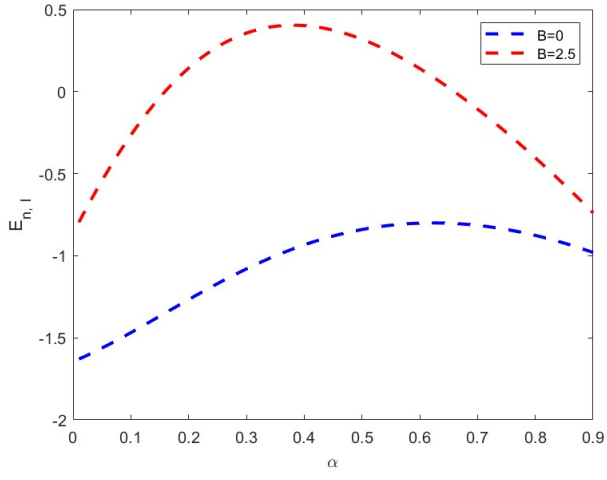

Figure 2: $E_{n,\ell}$ of the system versus α for $n = 0$.

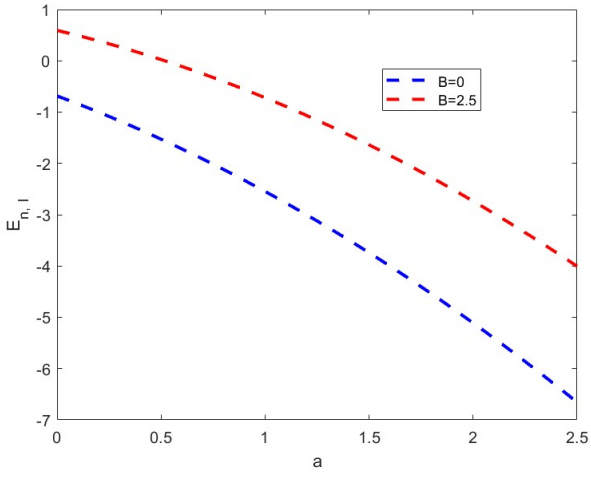

Figure 3: $E_{n,\ell}$ of the system versus a for $n = 0$.

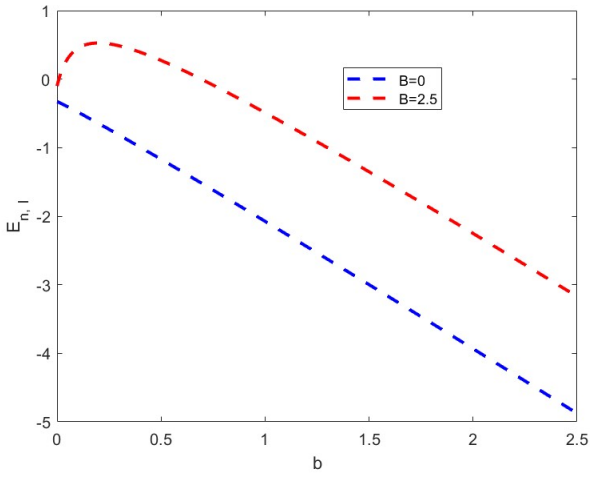

Figure 4: $E_{n,\ell}$ of the system versus b for $n = 0$.

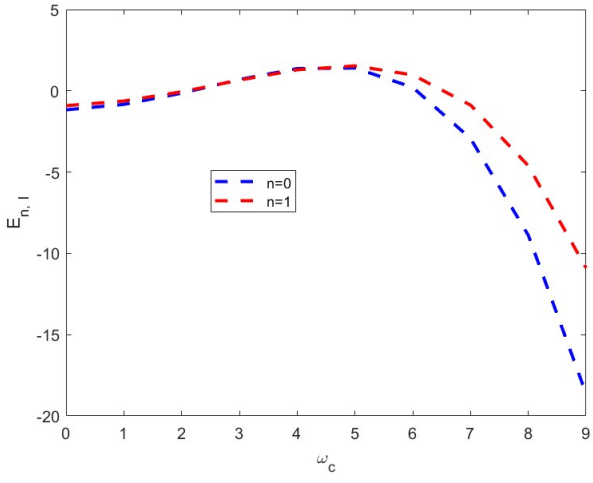

Figure 5: $E_{n,\ell}$ versus the cyclotron frequency.

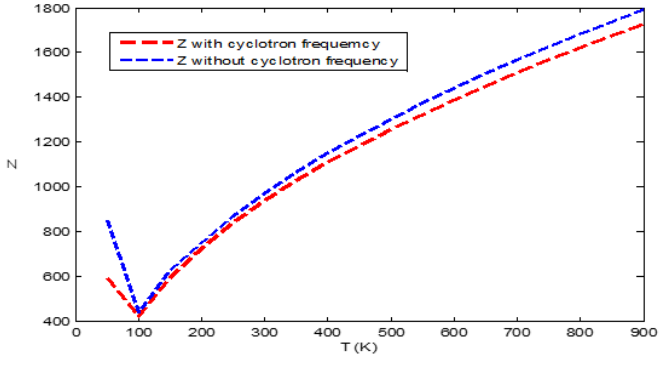

Figure 6: Vibrational partition function with cyclotron frequency and without cyclotron frequency as a function of temperature.

tightened. The presence of CF absorbed energy thereby reducing the negativity of the energy. This effect is in line with the

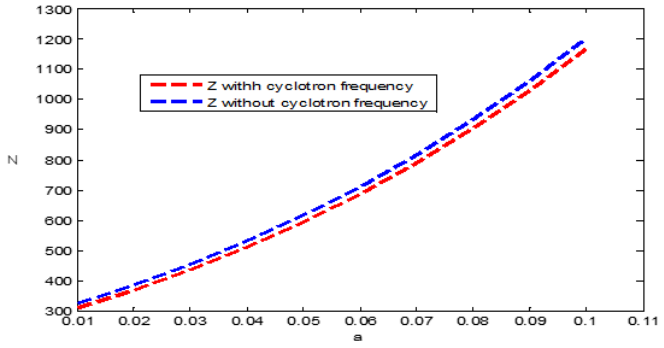

Figure 7: Vibrational partition function with cyclotron frequency and without cyclotron frequency as a function of the potential strength a.

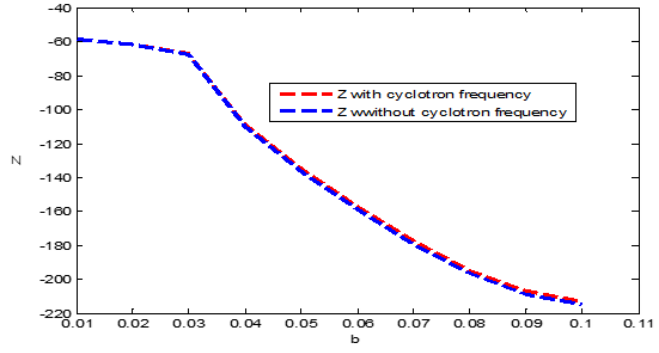

Figure 8: Vibrational partition function with cyclotron frequency and without cyclotron frequency as a function of the potential strength b.

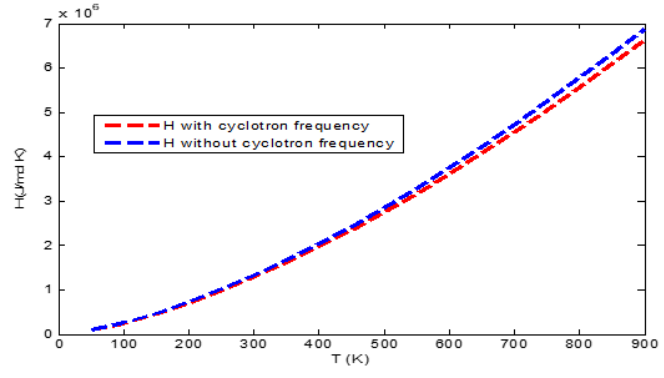

Figure 9: Vibrational enthalpy versus temperature with and without cyclotron frequency.

system of hydrogen atom obeying the energy system in quantum mechanics. Figure 2 represents the energy of the system as a function of α in the presence of CF and in the absence of CF. The presence of the CF increases energy of the system significantly thereby restricting the movement of electron. With the presence of the CF, the energy rises as the α increases from zero. At some values of α the energy attains a maximum and have a turning point. At this level, an increase in α leads to a

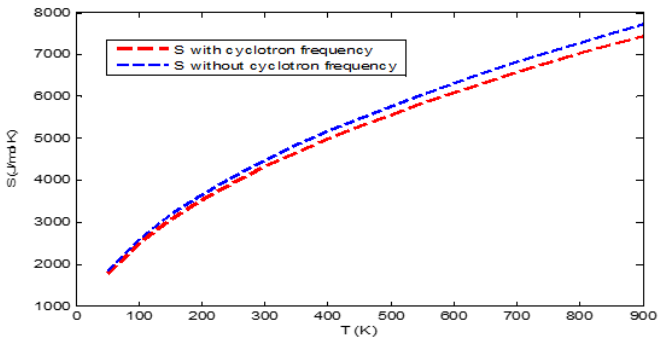

Figure 10: Vibrational entropy versus temperature with and without the cyclotron frequency.

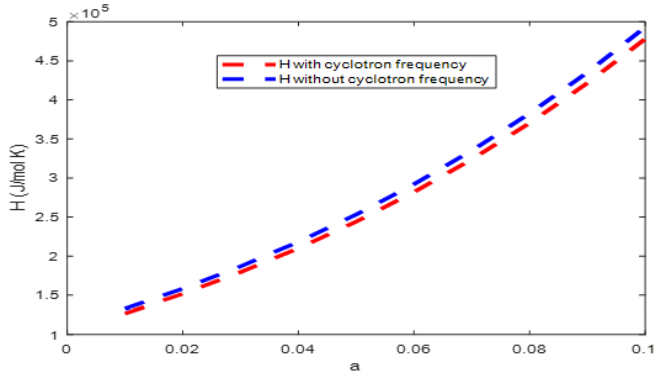

Figure 11: Vibrational enthalpy as a function of the parameter a.

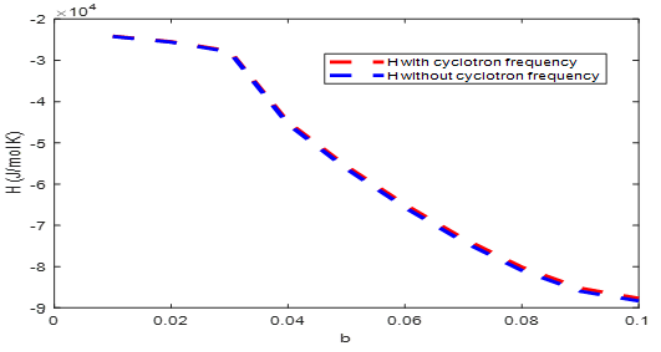

Figure 12: Vibrational enthalpy as a function of the parameter b.

decrease in energy making the energy more bounded. The initial increase in energy is due to Landau quantization which add additional confinement. As α becomes bigger, the Coulomb interaction weakens which shifts the dominant effect leading to decrease in energy. Figure 3 examine the effect of a on the energy in the presence and absence of the CF. As the parameter a increases, the energy of the system becomes more negatively creating more space for the movement of electron. However, in the presence of the CF, though the energy reduces with increase in a, the energy is higher than in the absence of the CF.

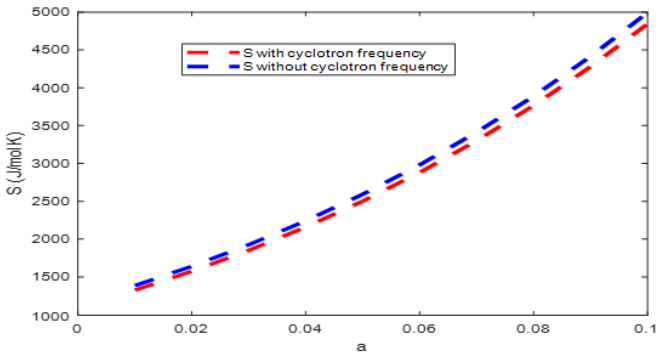

Figure 13: Vibrational entropy as a function of the parameter a.

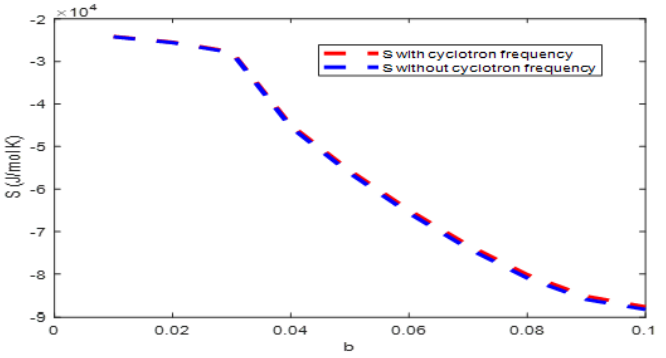

Figure 14: Vibrational entropy as a function of the parameter b.

Table 1: Vibrational G and vibrational C_p for various temperatures with $m = \hbar = q = 1$, $a = 0.05$, $b = 0.25$ and $\alpha = 0.5$.

T	$-G$ (B=0)	$-G$ (B=0.01)	C_p (B=0)	C_p (B=0.01)
050	2812.694041	2803.244051	4.157086869	4.157086033
100	5909.314740	5890.432084	4.157019289	4.157019009
150	9114.693229	9086.377903	4.157007765	4.157007616
200	12390.69890	12352.95089	4.157003986	4.157003887
250	15719.22240	15672.04172	4.157002343	4.157002271
300	19089.59758	19032.98423	4.157001500	4.157001437
350	22494.77664	22428.73061	4.157001008	4.157000964
400	25929.75039	25854.27168	4.157000706	4.157000677
450	29390.77349	29305.86210	4.157000513	4.157000481
500	32874.93878	32780.59471	4.157000386	4.157000357
550	36379.92385	36276.14711	4.157000290	4.157000263
600	39903.83050	39790.62107	4.157000210	4.157000195
650	43445.07810	43322.43598	4.157000162	4.157000148
700	47002.32993	46870.25515	4.157000134	4.157000110
750	50574.44087	50432.93340	4.157000098	4.157000086
800	54160.41874	54009.47861	4.157000068	4.157000061
850	57759.39572	57599.02291	4.157000065	4.157000043
900	61370.60623	61200.80073	4.157000051	4.157000023

Figure 4 shows the effect of the parameter b on energy with the presence and absence of the CF. An increase in the parameter b leads to a decrease in energy for both the presence and absence of the CF. Figure 5 represents the variation of energy against the CF for the ground state and the first excited state. As the CF increases from zero, the energy at the ground state and at the first excited state respectively, increases gradually and attains a maximum when the magnetic field is 5T, the energy then decreases monotonically. This suggests that the system confines the particle or bound to impurity. Before the decrease in energy, the energy at the ground state and at the first excited state are the same. In Figure 6, the Z increases as the temperature rises from 100K upward. As the temperature gets higher, the system accesses more energy states and the exponential term becomes less negative which means higher energy states become very populated and significantly accessible. This leads to increase in the Z. However, at low temperatures, only the low energy states are populated due to higher energy state which have exponentially small probabilities making the Z small. This effect affects both the Z obtained with CF and the one obtained without CF. However, the Z obtained with CF is lower than the Z obtained without CF at all temperatures. In quantum statistical mechanics, the presence of magnetic field causes the splitting of energy level and changes in degeneracy due to Zeeman effect. The reduction in degeneracy effectively alters the Z. The inclusion of the magnetic field lifted the degeneracies resulting to less probable of higher energy states because of Boltzmann factor. Figure 7 shows the vibrational Z as a function of the potential parameter a with the presence and absence of CF. The Z both with the presence and without the presence of CF respectively, rises as a increases linearly. The vibrational Z with CF is lower than the vibrational Z without the CF for all values of a. Figure 8 shows the effects of b on the vibrational Z in the presence and absence of the CF. The behaviour of the parameter b on the partition function is contrary to the behaviour of a on the Z. However, the Z in the presence

Table 2: Vibrational G and vibrational C_p for various a with $m = \hbar = q = 1$, $T = 100K$, $b = 0.25$ and $\alpha = 0.5$.

a	$-G$ (B=0)	$-G$ (B=0.01)	C_p (B=0)	C_p (B=0.01)
0.01	5605.061489	5585.899572	4.157013483	4.157013018
0.02	5681.543277	5662.447986	4.157015194	4.157014782
0.03	5757.751077	5738.725247	4.157016723	4.157016350
0.04	5833.676413	5814.721760	4.157018077	4.157017751
0.05	5909.314740	5890.432084	4.157019289	4.157019009
0.06	5984.664691	5965.854108	4.157020379	4.157020121
0.07	6059.727421	6040.988418	4.157021324	4.157021096
0.08	6134.506095	6115.837716	4.157022174	4.157021972
0.09	6209.005419	6190.406368	4.157022919	4.157022747
0.10	6283.231323	6264.700016	4.157023588	4.157023427

Table 3: Vibrational G and vibrational C_p for various b with $m = \hbar = q = 1$, $a = 0.25$, $T = 100K$ and $\alpha = 0.5$.

b	$-G$ (B=0)	$-G$ (B=0.01)	C_p (B=0)	C_p (B=0.01)
0.01	3391.284013	3388.494963	4.157015920	4.157017816
0.02	3446.516126	3442.671490	4.156973766	4.156975896
0.03	3565.434523	3559.408412	4.156885596	4.156888005
0.04	3931.170770	3923.121273	4.156958635	4.156959869
0.05	4088.631215	4079.874319	4.156969448	4.156970410
0.06	4224.783572	4215.254835	4.156963544	4.156964285
0.07	4356.635562	4346.259896	4.156955915	4.156956427
0.08	4490.644442	4479.370367	4.156950665	4.156950907
0.09	4629.876962	4617.692821	4.156948886	4.156948880
0.10	4775.648437	4762.586831	4.156950510	4.156950282

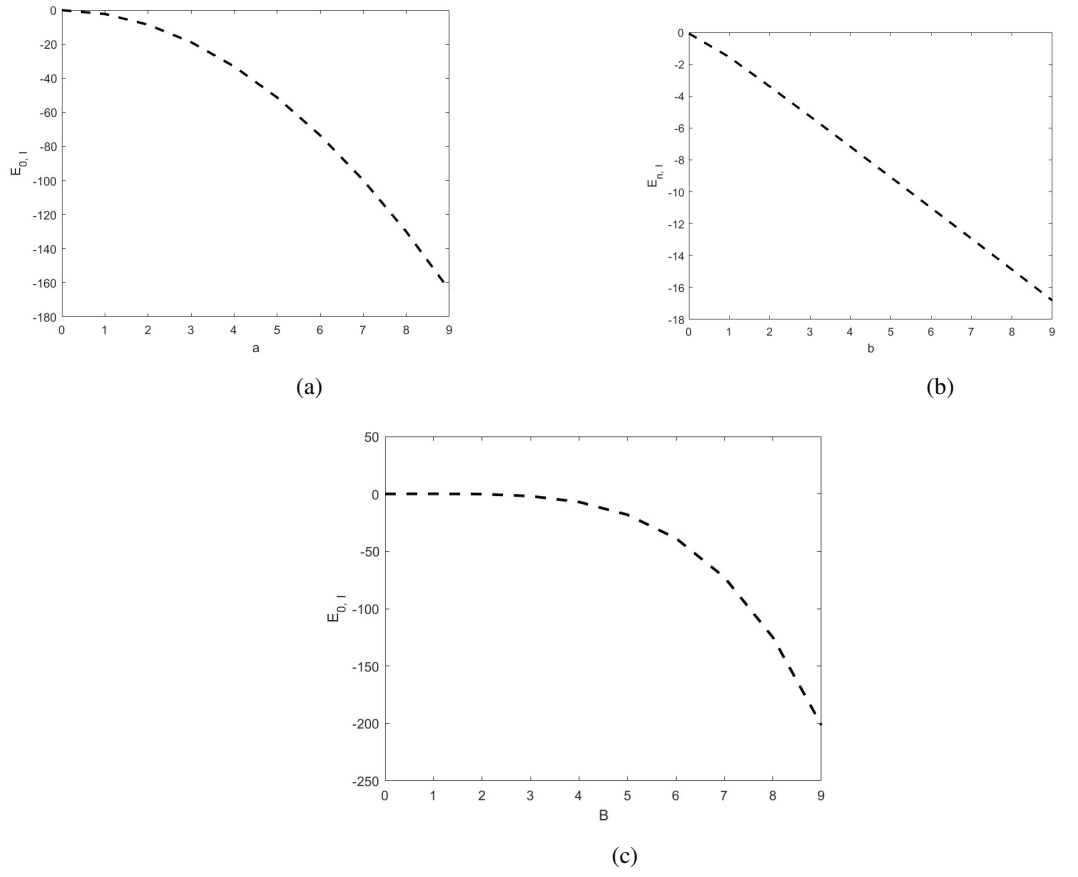

Figure 15: Variation of ground state energy against the potential parameter a (a), potential parameter b (b) and the magnetic field B (c).

and absence of CF as a function of b are closer compare to the variation in Figure 7.

As the temperature rises, the vibrational H both with the presence of CF and the absence of CF increases monotonically taking the same shape and direction as shown in Figure 9. Enthalpy as a TP and internal energy of a system are directly related to one another. The internal energy significantly depends on temperature. A rise in temperature leads to a fast movement of molecules which thus, increases the kinetic energy. Since H is directly related to internal energy which also depends on the temperature, the enthalpy therefore increases. At lower temperatures, the enthalpies are closer. However, as the temperature increases, there is discrepancy between the enthalpy with CF and the enthalpy without cyclotron frequency. The enthalpy obtained with CF at various temperatures is lower than the H obtained without the effect of CF. This means that the presence of magnetic field reduces the enthalpy of a system. With the presence of cyclotron frequency, the magnetic field introduced magnetization energy which alters the internal energy by the alignment of the magnetic dipoles. This situation reduces the energy of the system leading to a reduction in H. An increase in temperature leads to increase in entropy both with CF and without CF as represented in Figure 10. The entropies increase as the temperature rises. When the temperature of a system rises, its thermal energy also rises leading to increase in molecular motion. This results to a more disorderliness of the system that causes expansion in the range of accessible microstates. With increase in the number of microstate due to disorderliness of the system, the entropy increases. The two entropies are closer at lower temperatures but dispersed as the temperature increases to higher values. meanwhile, the entropy obtained without the influence of the CF is higher than the entropy obtained under the influence of CF at a every temperature. Including CF in a system means introducing magnetic field in the system. With the presence of magnetic field, the magnetic moments (spins) of the particles aligned is a direction. This causes a reduction in the randomness and the number of possible microstates in the system leading to entropy reduction.

In Figure 11, the enthalpy with cyclotron frequency and without CF respectively rises as the parameter a increases linearly. At every value of a, the enthalpy without the CF is higher than the enthalpy with CF. As a increases, the discrepancy between the enthalpies increases. In Figure 12, the enthalpy with CF and without CF respectively decreases as the parameter b increases linearly. At every value of b, the enthalpy without the CF is higher than the enthalpy with CF. The effect of b on enthalpy is contrary to the effect of a on enthalpy. Figure 13 represents entropy with cyclotron frequency and without CF

respectively as a function of the parameter a. The features observed in Figure 11 are also observed in Figure 13. Figure 14 represents entropy with CF and without CF respectively as a function of the parameter b. The features observed in Figure 12 are also observed in Figure 14. Table 1 presents data on vibrational G and vibrational C_p as functions of temperature (T), both in the presence and absence of cyclotron frequency. The values of G decrease with temperature from -2812.69 at 50 K to -61370.61 at 900K (with CF). A similar trend is observed in the presence of CF, but the values are slightly higher. This indicates that the presence of CF results in slightly higher Gibbs free energy values across all temperatures. The differences between the two datasets are relatively small but consistent. For instance, at 300K, the values are -19089.60 (without CF) and -19032.98 (with CF), showing only a marginal increase due to CF. This suggests that the effect of the CF on G is subtle but persistent. The heat capacity values remain nearly constant across all temperatures, approximately 4.157 in both cases. suggesting that vibrational contributions dominate and do not change significantly with temperature. There is an extremely small decrease in C values as temperature rises. The presence of cyclotron frequency has a minor effect on C_p, with values being slightly lower compared to the absence of CF. The effect of the CF is more pronounced in G than in heat capacity.

Table 2 presents data on vibrational G and vibrational C_p as a function of a parameter a in the presence and absence of CF. Both sets of values (with and without CF) decrease as the parameter a increases from 0.01 to 0.10. The presence of the CF consistently results in slightly higher G values compared to when it is absent. The difference between the two datasets remains relatively small but increases gradually with the parameter a. The C_p values remain relatively constant across the range of the parameter a. The differences between values in the presence and absence of the CF are extremely small, indicating minimal influence on vibrational C_p. The values exhibit a very slow downward trend but are nearly identical in both conditions. The minimal change in heat capacity implies that vibrational modes remain largely unaffected by the presence of the cyclotron frequency in terms of their ability to store heat. Table 3 presents data on vibrational G and vibrational C_p as a function of a parameter b with and without the influence of CF. In both cases (with and without CF), G increases as the parameter b increases from 0.01 to 0.10. The values of G are consistently higher in the presence of CF compared to its absence, indicating that the cyclotron effect leads to an increase in vibrational G. The increase in G is not linear; it shows a more pronounced rise beyond 0.03. The vibrational C_p values remain nearly constant across the range of the parameter b, with very slight variations. The differences between the two cases (with and without CF) are almost negligible regardless of the cyclotron effect. This suggests that CF does not significantly impact vibrational C_p. However, the value of the vibrational C_p with the present of the CF are slightly higher than their counter parts without the CF. The data suggests that the energy behavior is more affected by the CF than the C_p.

Figure 15 presents the variation of the ground state energy against the potential parameters. Figure 15(a) shows ground state energy against a with $b = B = 0$, (b) is energy against b with $a = B = 0$ while (c) is energy against the magnetic field B with $a = n = 0$. In all the cases, the energy decreases as the parameter increases and is completely bounded. The rate of decrease varies from parameter to parameter. The consistent decrease in the ground state energy across the three parameters suggests that increasing a, b or B enhances confinement or effective binding in a way that stabilizes the particle in a lower energy state. This behaviour is model-specific and might involve nontrivial potential shape or magnetic interactions. The heat capacity remains low or nearly constant even as temperature increases. This means that the system's ability to absorb and store thermal energy is limited. When the vibrational energy levels are widely spaced, even at higher temperatures, most particles remain in lower states. This limit the increase in the internal energy with temperature leading to low/constant heat capacity.

The physical relevance of this study to quantum dots, Landau levels and spintronic devices. The potential model in this study incorporates a magnetic field via the cyclotron frequency which is also fundamental to quantum system. The model mimics the parabolic confinement which are used in quantum dots. The magnetic field modifies the spacing of energy levels thereby replicating the magneto-optical properties of quantum dots. The presence of the cyclotron frequency increases the energy levels, closely paralleling Landau level formation in 2D electron gases such as in graphene. The turning point in the variation of energy against the screening parameter behaviour is reminiscent of transitions between quantized Landau levels. The Landau quantization arises from charged particles in a magnetic field. The magnetic fields influence spin alignment and spin splitting (Zeeman effect). The reduction in entropy and the altering in the partition function indicates spin polarization that is a key principle in spintronics. The system can model how magnetic control of entropy and energy levels can influence information storage in the spin-based devices. The magnetic field modifies the effective potential by tightening confinement for small r and broadening the well. This shift the equilibrium position and depth of the potential well, leading to higher energy eigenvalues and altered wave functions. Beyond the introduction of the cyclotron frequency, the magnetic field changes the curvature of the potential well, lifts degeneracies (Zeeman effect), modifies the spacing as well as the density of states (Landau-like quantization). As the magnetic field tends to zero, the potential (1) tends to the exponential-type potential of the form:

$$V(r) = -\frac{a}{1-e^{-\alpha r}} - \frac{b}{(1-e^{-\alpha r})^2}, \tag{38}$$

and the energy becomes lower as shown in Figures 1 to 4.

6. Conclusion

This study evaluates the influence of CF on the energy levels of the system and some TP. The energy levels rise in the presence of the CF incorporating a magnetic field which absorbed the energy. The presence of the CF in turn lower the Z and the

TP indicating a revised behaviour to that of the energy levels. The parameters a and b respectively portray a contrast effect on the energy as well as the TP. The study shows a thorough understanding of magnetic field influencing a quantum system via CF. The findings of this study are applicable in semiconductor science (in quantum wells and dots), Magnetic confinement in plasma (fusion energy), quantum computing (magnetic quantum computing), and thermodynamic quantum systems (thermodynamic stability in quantum statistical mechanics).

Data availability

All relevant data are within the manuscript.

References

[1] C. O. Edet, U. S. Okorie, G. Osobonye, A. N. Ikot, G. J. Rampho & R. Sever, "Thermal properties of Deng-Fan-Eckart potential model using Poisson summation approach", J. Math. Chem. **58** (2020) 989. https://doi.org/10.1007/s10910-020-01107-4.

[2] I. B. Okon, O. O. Popoola, E. Omugbe, A. D. Antia, C. N. Isonguyo & E. E. Ituen, "Thermodynamic properties and bound state solutions of Schrödinger equation with Möbius square plus screened-Kratzer potential using Nikiforov-Uvarov method", Comp. Theor. Chem. **1196** (2021) 113132. https://doi.org/10.1016/j.comptc.2020.113132.

[3] A. N. Ikot, U. S. Okorie, R. Sever & G. J. Rampho, "Eigensolution, expectation values and thermodynamic properties of the screened Kratzer potential", Eur. Phys. J. Plus **134** (2019) 386. https://doi.org/10.1140/epjp/i2019-12783-x.

[4] G. J. Rampho, A. N. Ikot, C. O. Edet & U. S. Okorie, "Energy spectra and thermal properties of diatomic molecules in the presence of magnetic and AB fields with improved Kratzer potential", Mol. Phys. **119** (2021) e1821922. https://doi.org/10.1080/00268976.2020.1821922.

[5] K. O. Emeje, C. A. Onate, I. B. Okon, E. Omugbe, E. S. Eyube, D. B. Olanrewaju & E. Aghemenloh, "Eigensolution and thermodynamic properties of standard Coulombic potential", J. Low Temp. Phys. **215** (2024) 109. https://doi.org/10.1007/s10909-024-03074-5.

[6] Y. Jiang, L. Liu, J. Yan & Z. Wu, "Room-to-low temperature thermomechanical behavior and corresponding constitutive model of liquid oxygen compatible epoxy composites", Comp. Sci. Techn. **245** (2024) 110357. https://doi.org/10.1016/j.compscitech.2023.110357.

[7] M. Habibinejad, R. Khordad & A. Ghanbari, "Specific heat at constant pressure, enthalpy and Gibbs free energy of boron nitride (BN) using q-deformed exponential-type potential", Physica B **613** (2021) 412940. https://doi.org/10.1016/j.physb.2021.412940.

[8] R. Khordad & A. Ghanbari, "Theoretical prediction of thermal properties of K2 diatomic molecule using generalized Möbius square potential", Int. J. Thermophys. **42** (2021) 115. https://doi.org/10.1007/s10765-021-02865-2.

[9] C. A. Onate, I. B. Okon, E. Omugbe, E. S. Eyube, B. A. Al-Asbahi, Y. A. Kumar, K. O. Emeje, E. Aghemenloh, A. R. Obasuyi, V. O. Obaje & T. O. Etchie, "Theoretical prediction of molar entropy of modified shifted Morse potential for gaseous molecules", Chem. Phys. **582** (2024) 112294. https://doi.org/10.1016/j.chemphys.2024.112294.

[10] E. S. Eyube, P. P. Notani & H. Samaila, "Analytical prediction of enthalpy and Gibbs free energy of gaseous molecules", Chem. Thermody. Thermal Analysis **6** (2022) 100060. https://doi.org/10.1016/j.ctta.2022.100060.

[11] K. O. Emeje, E. Aghemenloh & C. A. Onate, "Analytical determination of enthalpy, heat capacity and Gibbs free energy for nitrogen and iodine", Chem. Phys. Lett. **844** (2024) 141271. https://doi.org/10.1016/j.cplett.2024.141271.

[12] W. Song, N. Martsinovich, W. M. Heckl & M. Lackinger, "Thermodynamic of halogen bonded monolayer self-assembly at the liquid-solid interface", Chem. Commun. **50** (2014) 13465. https://doi.org/10.1039/C4CC06251E.

[13] K. I. Amano, T. Yoshidome, Y. Harano, K. Oda & M. Kinoshita, "Theoretical analysis on thermal stability of a protein focused on the water entropy", Chem. Phys. Lett. **474** (2009) 190. https://doi.org/10.1016/j.cplett.2009.04.025.

[14] N. M. Yunus, M. I. A. Mutalib, Z. Man, M. A. Bustam & T. Murugesan, "Solubility of CO2 in pyridinium based ionic liquids", Chem. Engr. J. **94** (2012) 189. https://doi.org/10.1016/j.cej.2012.02.033.

[15] N. P. Stadie, M. Murialdo, C. C. Ahn & B. Fultz, "Anomalous isosteric enthalpy of adsorption of methane on zeolite-templated carbon supporting information", J. Am. Chem. Soc. **135** (2013) 990. https://doi.org/10.1021/ja311415m.

[16] T. Zhang, G. S. Ellis, S. C. Ruppel, K. Milliken & R. Yang, "Effect of organic-matter type and thermal maturity on methane adsorption in shale-gas systems", Org. Geochem **47** (2012) 120. https://doi.org/10.1016/j.orggeochem.2012.03.012.

[17] S. A. Moses, J. P. Covey, M. T. Miecnikowski, B. Yan, B. Gadway, J. Ye & D. S. Jin, "Creation of a low entropy quantum gas of polar molecules in an optical lattice", Science **350** (2015) 659. https://doi.org/10.1126/science.aac640.

[18] S. Dastidar, C. J. Hawley, A. D. Dillon, A. D. Gutierrez-Perez, J. E. Spanier & A. T. Fafarman, "Quantitative phase-change thermodynamics and metastability of perovskite-phase cesium lead iodide", J. Phys. Chem. Lett. **8** (2017) 1278. https://doi.org/10.1021/acs.jpclett.7b00134.

[19] C. Tezcan & R. Sever, "A general approach for the exact solution of the Schrödinger equation", Int. J. Theor. Phys. **48** (2009) 337. https://doi.org/10.1007/s10773-008-9806-y.

[20] R. L. Greene & C. Aldrich, "Variational wave functions for screened Coulomb potential", Phys. Rev. A **14** (1976) 2363. https://doi.org/10.1103/PhysRevA.14.2363.

[21] C. A. Onate, J. A. Akinpelu, O. O. Ajani, B. B. Deji-Jinadu, F. O. Aweda, J. B. Fashae & O. O. Jegede, "Molar enthalpy and heat capacity for symmetric trigonometric Rosen-Morse plus Pöschl-Teller potential", South Afr. J. Chem. Eng. **51** (2025) 15. https://doi.org/10.1016/j.sajce.2024.10.007.

[22] S. H. Dong, R. Lemus & A. Frank, "Ladder operators for the Morse potential", Int. J. Quant. Chem. **86** (2002) 433. https://doi.org/10.1002/qua.10038.

[23] R. Khordad & H. R. Sedehi, "Thermodynamic properties of a double ring-shaped quantum dot at low and high temperatures", J. Low Temp. Phys. **190** (2018) 200. https://doi.org/10.1007/s10909-017-1831-x.

[24] S. H. Dong, "The SU(2) realization for the Morse potential and its coherent states", Can. J. Phys. **80** (2002) 129. https://doi.org/10.1139/p01-130.

[25] G. H. Liu, Q. C. Ding, C. W. Wang & C. S. Jia, "Unified non-fitting explicit formulation of thermodynamic properties for five compounds", J. Mol. Str. **1294** (2023) 136543. https://doi.org/10.1016/j.molstruc.2023.136543.

[26] S. H. Dong & M. Cruz-Irisson, "Energy spectrum for a modified Rosen-Morse potential solved by proper quantization rule and its thermodynamic properties", J. Math. Chem. **50** (2012) 881. https://doi.org/10.1007/s10910-011-9931-3.

[27] R. Khordad & A. Ghanbari, "Theoretical prediction of thermodynamic functions of TiC: Morse ring-shaped potential", J. Low Temp. Phys. **199** (2020) 1198. https://doi.org/10.1007/s10909-020-02368-8.

[28] R. Khordad & A. Ghanbari, "Analytical calculations of thermodynamic functions of lithium dimer using modified Tietz and Badawi-Bessis-Bessis potentials", Comput. Theor. Chem. **1155** (2019) 1. https://doi.org/10.1016/j.comptc.2019.03.019.

[29] S. H. Dong, M. Lozada-Cassou, J. Yu, F. Jimenez-Ángeles & A. L. Rivera, "Hidden symmetries and thermodynamic properties for a harmonic oscillator plus an inverse square potential", Int. J. Quant. Chem. **107** (2007) 366. https://doi.org/10.1002/qua.21103.

[30] M. L. Strekalov, "An accurate closed-form expression for the partition function of Morse oscillators", Chem. Phys. Lett. **439** (2007) 209. https://doi.org/10.1016/j.cplett.2007.03.052.

[31] C. S. Jia, R. Zeng, X. L. Peng, L. H. Zhang & Y. L. Zhao, "Entropy of gaseous phosphorus dimer", Chem. Eng. Sci. **190** (2018) 122. https://doi.org/10.1016/j.ces.2018.06.009.

[32] X. L. Peng, R. Jiang, C. S. Jia, L. H. Zhang & Y. L. Zhao, "Gibbs free energy of gaseous phosphorus dimer", Chem. Eng. Sci. **190** (2018) 122. https://doi.org/10.1016/j.ces.2018.06.027.

[33] C. S. Jia, C. W. Wang, L. H. Zhang, X. L. Peng, H. M. Tang, J. Y. Liu, Y. Xiong & R. Zeng, "Predictions of entropy for diatomic molecules and gaseous substances", Chem. Phys. Lett. **692** (2018) 57. https://doi.org/10.1016/j.cplett.2017.12.013.

[34] R. Jiang, C. S. Jia, Y. Q. Wang, X. L. Peng & L. H. Zhang, "Prediction of Gibbs free energy for the gases Cl2, Br2, and HCl", Chem. Phys. Lett. **726** (2019) 83. https://doi.org/10.1016/j.cplett.2019.04.040.

[35] C. S. Jia, J. Li, Y. S. Liu, X. L. Peng, X. Jia, L. H. Zhang, R. Jiang, X. P. Li, J. Y. Liu & Y. L. Zhao, "Predictions of thermodynamic properties for hydrogen sulfide", J. Mol. Liquid **315** (2020) 113751. https://doi.org/10.1016/j.molliq.2020.113751.

[36] M. H. Abdulameer, A. B. M. Ali, A. K. Nemah, P. Kanjariya, A. Rajiv, M. Agarwal, P. Kaur & A. A. Almehizia, "Prediction of molar entropy of gaseous molecules for a new Pöschl-Teller potential model", Int. J. Quant. Chem. **124** (2024) e27505. https://doi.org/10.1002/qua.27505.